

UDC: 519.6

## Analytical Approximation of a Nonlinear Model for Pest Control in Coconut Trees by the Homotopy Analysis Method

G. Suganya, R. Senthamarai<sup>a</sup>

Department of Mathematics, College of Engineering and Technology, SRM Institute of Science and Technology,  
Kattankulathur – 603 203, Tamil Nadu, India

E-mail: <sup>a</sup> [senthamr@srmist.edu.in](mailto:senthamr@srmist.edu.in)

Received 15.06.2022, after completion – 22.07.2022.

Accepted for publication 09.08.2022.

Rugose spiraling whitefly (RSW) is one of the major pests which affects the coconut trees. It feeds on the tree by sucking up the water content as well as the essential nutrients from leaves. It also forms sooty mold in leaves due to which the process of photosynthesis is inhibited. Biocontrol of pest is harmless for trees and crops. The experimental results in literature reveal that *Pseudomallada astur* is a potential predator for this pest. We investigate the dynamics of predator, *Pseudomallada astur*'s interaction with rugose spiralling whitefly, *Aleurodicus rugioperculatus* in coconut trees using a mathematical model. In this system of ordinary differential equation, the pest-predator interaction is modeled using Holling type III functional response. The parametric values are calculated from the experimental results and are tabulated. An approximate analytical solution for the system has been derived. The homotopy analysis method proves to be a suitable method for creating solutions that are valid even for moderate to large parameter values, hence we employ the same to solve this nonlinear model. The  $\hbar$ -curves, which give the admissible region of  $\hbar$ , are provided to validate the region of convergence. We have derived the approximate solution at fifth order and stopped at this order since we obtain a more approximate solution in this iteration. Numerical simulation is obtained through MATLAB. The analytical results are compared with numerical simulation and are found to be in good agreement. The biological interpretation of figures implies that the use of a predator reduces the whitefly's growth to a greater extent.

Keywords: mathematical model, *Pseudomallada astur*, rugose spiraling whitefly, coconut trees, homotopy analysis method,  $\hbar$ -curves

Citation: *Computer Research and Modeling*, 2022, vol. 14, no. 5, pp. 1093–1106.

## 1. Introduction

The coconut trees belong to the species of palm family that grows extensively in tropical climates. India ranks top in coconut and its allied products production with the southern states of the country contributing the most. The five major states, namely, Tamil Nadu, Kerala, Karnataka, Andhra Pradesh and Telangana, contribute around 90 percent of the country's coconut plantation. One of the major challenges which farmers face in bringing up these trees is pest that ruins the tree's growth as well as its coconut production. Rugose spiraling whitefly, an exotic pest affecting coconut trees since 2016 in India, feeds on the host plant by sucking up the water content as well as the essential nutrients from leaves. It inhibits the photosynthesis process by formation of sooty mold in leaves, which makes the tree less likely to get the sun's exposure. There are some management strategies to control RSW population such as spraying insecticides, usage of bio-pesticides & with the help of natural enemies [Elango, Nelson, Aravind, 2020; Elango, 2019; Sundararaj, Selvaraj, 2017]. In [Rao, Ramani, Bhagavan, 2020], N. C. Rao et al. investigated *Pseudomallada astur*'s functional response and its density-dependent feeding interaction with Rugose spiralling whitefly. Type III functional response was followed by all larval instars. It has been reported that *Pseudomallada astur* is a potential predator of whitefly infesting coconut palms. Field evaluation resulted in significantly low population of whitefly after inoculating the *Pseudomallada astur* eggs in the whitefly infected leaves [Chalapathi Rao et al., 2022].

The dynamics of population interaction can be analyzed using a mathematical model. In epidemiology, the formulation and notion of mathematical models have been explained [Allen et al., 2008]. The African cassava mosaic virus disease was examined using an epidemiological model that included vector population dynamics [Holt et al., 1997]. The dynamical behavior of a model for biocontrol of pests with Holling type II functional response has been analyzed in [Pathak, Maiti, 2012]. Modeling and analysis of Phytoplankton–Zooplankton–Nanoparticle dynamics has been studied in [Suganya, Senthamarai, 2022a]. The effect of the rugose spiraling whitefly on coconut trees has been analyzed. The results evoked that, controlling the contact rate with control measures can reduce the risk of healthy trees becoming infected and also the intensity of infection [Suganya, Senthamarai, 2022b]. To solve the nonlinear problems, there are many analytical methods to find an approximate analytical solution. Liao proposed the homotopy analysis method (HAM), which overcomes the restrictions of perturbation techniques while solving the nonlinear problems. It allows us to fine-tune the rate of convergence and the convergence region by varying an auxiliary parameter  $\hbar$ . The convergence of the HAM series solution is ensured by an appropriate choice of auxiliary linear operator, initial conditions and the auxiliary parameter  $\hbar$  [Liao, 2003; Liao, 2013; Liao, 2004]. HAM has been applied to estimate the analytical approximation of the HIV viral dynamic model [Naik, Zu, Ghoreishi, 2020a]. The collocation method (CM), the homotopy perturbation method (HPM) and HAM have been applied for unsteady time-dependent incompressible Newtonian fluid flow between two parallel plates [Shirkhani et al., 2018]. Stability analysis and an approximate solution of the SIR epidemic model have been carried out by using the homotopy analysis method [Naik, Zu, Ghoreishi, 2020b]. A modified nonlinear epidemiological model of computer viruses has been illustrated and solved by the homotopy analysis method [Noeiaghdam, Suleman, Budak, 2018].

In this paper, we propose a mathematical model describing the interaction of a predator with a rugose spiraling whitefly in coconut trees. The parametric values are framed based on data given in [Elango, Nelson, Aravind, 2020; Rao, Ramani, Bhagavan, 2020; Chalapathi Rao et al., 2022]. We apply the homotopy analysis method to solve our model since it is independent of large or small parameters. The validation of our solution is shown by  $\hbar$ -curves and error tables.

## 2. Mathematical Formulation

In [Suganya, Senthamarai, 2022b], the analysis has been carried out for the interaction between a rugose spiraling whitefly and coconut trees. The mathematical model in [Pathak, Maiti, 2012] studied the dynamics of biocontrol of pest using a virus with Holling type II interaction. Hence, we propose a mathematical model to study the dynamics of whitefly population in the presence of its predator. Let  $E$  denote the number of coconut leaves,  $F$  the *Aleurodicus rugioperculatus* (whitefly) eggs per leaf and  $G$  the *Pseudomallada astur* (predator) eggs per leaf:

$$\frac{dE}{dt} = rE - \alpha EF, \quad (1)$$

$$\frac{dF}{dt} = \beta \alpha EF - \frac{aF^2G}{b^2 + F^2} - \zeta F, \quad (2)$$

$$\frac{dG}{dt} = \frac{acF^2G}{b^2 + F^2} - \omega G + \eta \quad (3)$$

with the initial conditions

$$E(0) > 0, \quad F(0) > 0, \quad G(0) \geq 0. \quad (4)$$

The parameters in our model are defined as follows:

- Let  $r$  be the growth rate of coconut leaves and  $\alpha$  be the infection rate due to the interaction of the whitefly.
- Let  $\beta$  denote the growth rate of the whitefly,  $b$  the half saturation constant and  $\zeta$  the death rate of the whitefly.
- Let  $\eta$  be the number of predator eggs added to the system,  $a$  be the predation rate of the whitefly per predator,  $c$  the growth rate of predator, and  $\omega$  the death rate of predator.
- The whitefly-predator interaction is modeled using Holling type III functional response since the experimental data [Rao, Ramani, Bhagavan, 2020] resulted in type III functional response in all stages of predator.

Now, we use the following scaling to nondimensionalize the system:

$$L = \frac{E}{s}, \quad W = \frac{F}{x}, \quad G = \frac{A}{\eta}, \quad \tau = t\omega, \quad f = \frac{r}{\omega}, \quad n = \frac{\zeta}{\omega}, \quad u^2 = \frac{b^2}{x^2},$$

$$x = \frac{\omega}{\alpha}, \quad s = \frac{\eta}{\beta}, \quad m = \frac{\alpha\eta}{\omega}, \quad p = \frac{am}{\omega}, \quad q = \frac{ac}{\omega}, \quad g = \frac{n}{\zeta}.$$

The nondimensional system is given by

$$\frac{dL}{d\tau} = fL - LW, \quad (5)$$

$$\frac{dW}{d\tau} = mLW - \frac{pW^2A}{u^2 + W^2} - nW, \quad (6)$$

$$\frac{dA}{d\tau} = \frac{qW^2A}{u^2 + W^2} - A + g \quad (7)$$

with the initial conditions

$$L(0) > 0, \quad W(0) > 0, \quad A(0) \geq 0, \quad (8)$$

where  $L$  denotes the coconut leaves,  $W$  the whitefly eggs, and  $A$  the predator eggs.

### 3. Approximate Analytical Expression

The homotopy analysis method was proposed by Liao [Liao, 2003; Liao, 2013; Liao, 2004] which is a powerful technique to solve the nonlinear problems and to obtain a series of solutions. The HAM methodology, unlike many analytical methods, can be used to find valid solutions even to problems that are highly nonlinear. The rate of convergence and the region of the solution series can be adjusted by changing the auxiliary parameter  $\hbar$  present in the approximate solution. To construct a HAM solution, we denote

$$L_0 = L(0)e^{f\tau}, \quad (9)$$

$$W_0 = W(0)e^{-n\tau}, \quad (10)$$

$$A_0 = g - ge^{-\tau}, \quad (11)$$

as the initial approximation for  $L(\tau)$ ,  $W(\tau)$ ,  $A(\tau)$ .

We choose the auxiliary linear operators  $\Phi_1$ ,  $\Phi_2$ ,  $\Phi_3$  as

$$\Phi_1[L(\tau, \lambda)] = \frac{dL(\tau, \lambda)}{d\tau} + fL, \quad (12)$$

$$\Phi_2[W(\tau, \lambda)] = \frac{dW(\tau, \lambda)}{d\tau} + nW, \quad (13)$$

$$\Phi_3[A(\tau, \lambda)] = \frac{dA(\tau, \lambda)}{d\tau} + A - g, \quad (14)$$

with the property  $\Phi_1[c_1 e^{f\tau}] = 0$ ,  $\Phi_2[c_2 e^{-n\tau}] = 0$ ,  $\Phi_3[c_3 e^{-\tau} + g] = 0$ , where  $c_1$ ,  $c_2$ ,  $c_3$  are constant coefficients.

Define the nonlinear operators as follows:

$$N_1[L, W, A] = \dot{L} - fL + LW, \quad (15)$$

$$N_2[L, W, A] = \dot{W} - mLW + \frac{pW^2A}{u^2 + W^2} + nW, \quad (16)$$

$$N_3[L, W, A] = \dot{A} - \frac{qW^2A}{u^2 + W^2} + A - g. \quad (17)$$

The zero-order deformation equations, according to Liao, can be defined as

$$(1 - \lambda)\Phi_1[L(\tau, \lambda) - L_0(\tau)] = \lambda\hbar H_1(\tau)N_1[L, W, A], \quad (18)$$

$$(1 - \lambda)\Phi_2[W(\tau, \lambda) - W_0(\tau)] = \lambda\hbar H_2(\tau)N_2[L, W, A], \quad (19)$$

$$(1 - \lambda)\Phi_3[A(\tau, \lambda) - A_0(\tau)] = \lambda\hbar H_3(\tau)N_3[L, W, A], \quad (20)$$

where  $\lambda \in [0, 1]$  is the embedding parameter,  $\hbar \neq 0$  is a nonzero auxiliary parameter,  $H(t) \neq 0$  is an auxiliary function, and  $\Phi$  is an auxiliary linear operator.

It is essential to note that in HAM one has a considerable deal of flexibility in selecting auxiliary unknowns.

When  $\lambda = 0$  and  $\lambda = 1$ , it follows that:

$$L(\tau; 0) = L_0(\tau) \quad \text{and} \quad L(\tau; 1) = L(\tau), \quad (21)$$

$$W(\tau; 0) = W_0(\tau) \quad \text{and} \quad W(\tau; 1) = W(\tau), \quad (22)$$

$$A(\tau; 0) = A_0(\tau) \quad \text{and} \quad A(\tau; 1) = A(\tau). \quad (23)$$

As  $\lambda$  tends to rise from 0 to 1, the terms  $L(\tau, \lambda)$ ,  $W(\tau, \lambda)$  and  $A(\tau, \lambda)$  change from the initial guess to the final solution. With regard to  $\lambda$ , we can expand these terms in Taylor series as follows:

$$L(\tau; \lambda) = L_0(\tau) + \sum_{i=1}^{\infty} L_i(\tau)\lambda^i, \quad (24)$$

$$W(\tau; \lambda) = W_0(\tau) + \sum_{i=1}^{\infty} W_i(\tau)\lambda^i, \quad (25)$$

$$A(\tau; \lambda) = A_0(\tau) + \sum_{i=1}^{\infty} A_i(\tau)\lambda^i, \quad (26)$$

where

$$L_i = \left. \frac{1}{i!} \frac{\partial^i L(\tau; \lambda)}{\partial \lambda^i} \right|_{\lambda=0}, \quad (27)$$

$$W_i = \left. \frac{1}{i!} \frac{\partial^i W(\tau; \lambda)}{\partial \lambda^i} \right|_{\lambda=0}, \quad (28)$$

$$A_i = \left. \frac{1}{i!} \frac{\partial^i A(\tau; \lambda)}{\partial \lambda^i} \right|_{\lambda=0}. \quad (29)$$

The series converges at  $\lambda = 1$  if the auxiliary linear operator, the initial guess, the auxiliary parameter and the auxiliary function are all chosen suitably. Then we have

$$L(\tau) = L_0(\tau) + \sum_{i=1}^{\infty} L_i(\tau), \quad (30)$$

$$W(\tau) = W_0(\tau) + \sum_{i=1}^{\infty} W_i(\tau), \quad (31)$$

$$A(\tau) = A_0(\tau) + \sum_{i=1}^{\infty} A_i(\tau). \quad (32)$$

We can obtain the so-called  $i^{\text{th}}$  order deformation equation by differentiating (18)–(20)  $i$  times with regard to the embedding parameter  $\lambda$ , then setting  $\lambda = 0$  and then dividing them by  $i!$

$$\Phi_1[L_i(\tau) - \Omega_i L_{i-1}(\tau)] = \hbar M_{1,i}(L_{i-1}(\tau)), \quad (33)$$

$$\Phi_2[W_i(\tau) - \Omega_i W_{i-1}(\tau)] = \hbar M_{2,i}(W_{i-1}(\tau)), \quad (34)$$

$$\Phi_3[A_i(\tau) - \Omega_i A_{i-1}(\tau)] = \hbar M_{3,i}(A_{i-1}(\tau)) \quad (35)$$

subject to the initial condition

$$L_i(0) = 0, \quad W_i(0) = 0, \quad A_i(0) = 0, \quad (36)$$

where

$$M_{1,i}(\tau) = \frac{dL_{i-1}(\tau)}{d\tau} - fL_{i-1} + \sum_{j=0}^{i-1} L_j(\tau)W_{i-1-j}(\tau), \quad (37)$$

$$M_{2,i}(\tau) = \frac{dW_{i-1}(\tau)}{d\tau} u^2 + \sum_{j=0}^{i-1} \frac{dW_{i-1-j}(\tau)}{d\tau} \sum_{k=0}^j W_k W_{j-k} + p \sum_{j=0}^{i-1} A_{i-1-j} \sum_{k=0}^j W_k W_{j-k} -$$

$$-mu^2 \sum_{j=0}^{i-1} L_j W_{i-1-j} + nu^2 W_{i-1} - m \sum_{j=0}^{i-1} L_{i-1-j} \sum_{k=0}^j W_{j-k} \sum_{y=0}^k W_y W_{k-y} + n \sum_{j=0}^{i-1} W_{i-1-j} \sum_{k=0}^j W_k W_{j-k}, \quad (38)$$

$$M_{3,i}(\tau) = \frac{dA_{i-1}(\tau)}{d\tau} u^2 + \sum_{j=0}^{i-1} \frac{dA_{i-1-j}(\tau)}{d\tau} \sum_{k=0}^j W_k W_{j-k} - q \sum_{j=0}^{i-1} A_{i-1-j} \sum_{k=0}^j W_k W_{j-k} + A_{i-1} u^2 + \\ + \sum_{j=0}^{i-1} A_{i-1-j} \sum_{k=0}^j W_k W_{j-k} - (1 - \Omega_i) g u^2 - g \sum_{j=0}^{i-1} W_{i-1-j} W_j \quad (39)$$

and

$$\Omega_i = \begin{cases} 0, & i \leq 1, \\ 1, & i > 1. \end{cases} \quad (40)$$

For  $i \geq 1$ , the  $i^{\text{th}}$ -order deformation equation becomes

$$L_i(\tau) = \Omega_i L_{i-1}(\tau) + \hbar \int_0^\tau M_{1,i}(t) dt, \quad (41)$$

$$W_i(\tau) = \Omega_i W_{i-1}(\tau) + \hbar \int_0^\tau M_{2,i}(t) dt, \quad (42)$$

$$A_i(\tau) = \Omega_i A_{i-1}(\tau) + \hbar \int_0^\tau M_{3,i}(t) dt. \quad (43)$$

In this way, we may easily derive  $L_i$ ,  $W_i$ ,  $A_i$  for  $i \geq 1$  at the  $M^{\text{th}}$  order and obtain

$$L(\tau) = \sum_{i=0}^M L_i(\tau), \quad W(\tau) = \sum_{i=0}^M W_i(\tau) \quad \text{and} \quad A(\tau) = \sum_{i=0}^M A_i(\tau). \quad (44)$$

The approximate analytical solution of the system for the parametric value  $f = 0.09$ ,  $n = 0.67$ ,  $m = 0.01$ ,  $p = 0.063$ ,  $q = 0.6$ ,  $g = 10$ ,  $u = 0.33$  is given by

$$L(\tau) = 0.03e^{0.09\tau} + 0.06931034482\hbar - 0.06931034482\hbar e^{-0.58\tau} + 0.052777496520\hbar^2 - \\ - 0.03118965517\tau\hbar^2 + 0.02990619719\hbar^2 e^{0.09\tau} - 0.04003269916\hbar^2 e^{-0.58\tau} - \\ - 0.0001611435898\hbar^2 e^{-2.25\tau} - 7.703970287 \cdot 10^{-7}\hbar^2 e^{-1.83\tau} + 0.01908169241\hbar^2 e^{-1.25\tau} - \\ - 0.03465517238\hbar^2 e^{-0.67\tau} - 2.3110580577 \cdot 10^{-8}\hbar^2 e^{-0.49\tau}, \quad (45)$$

$$W(\tau) = 0.67e^{-0.67\tau} + 0.01794371830\hbar + 7.547896549 \cdot 10^{-7}\hbar e^{-0.58\tau} + 0.00009398843747\hbar e^{-1.92\tau} + \\ + 0.02417153845\hbar e^{-2.34\tau} - 0.04220999998\hbar e^{-1.34\tau} + 6.546137591 \cdot 10^{-6}\hbar^2\tau + \\ + 9.392966874 \cdot 10^{-6}\hbar^2 e^{-2.34\tau} + 2.537695406 \cdot 10^{-8}\hbar^2 e^{-1.92\tau} - 0.0002123600749\hbar^2 e^{-1.34\tau} - \\ - 0.001694549195\hbar^2 e^{-0.67\tau} - 6.377321895 \cdot 10^{-11}\hbar^2 e^{-0.58\tau} + 0.0003816511113\hbar^2 e^{-4.01\tau} + \\ + 0.003346585623\hbar^2 e^{-3.68\tau} + 3.017729677 \cdot 10^{-6}\hbar^2 e^{-3.59\tau} + 8.088843853 \cdot 10^{-6}\hbar^2 e^{-3.26\tau} + \\ + 5.989316815 \cdot 10^{-9}\hbar^2 e^{-3.17\tau} - 0.001396327942\hbar^2 e^{-3.01\tau} - 0.004489561122\hbar^2 e^{-2.86\tau} - \\ - 0.00004583299037\hbar^2 e^{-2.59\tau} + 2.299463458 \cdot 10^{-8}\hbar^2 e^{-2.25\tau} + 0.001381470689\hbar^2 e^{-2.01\tau} + \\ + 9.170726528 \cdot 10^{-11}\hbar^2 e^{-1.83\tau} + 0.0006803033077\hbar^2 e^{-1.67\tau} + 2.299463458 \cdot 10^{-8}\hbar^2 e^{-2.25\tau} + \\ + 0.001381470689\hbar^2 e^{-2.01\tau} + 9.170726528 \cdot 10^{-11}\hbar^2 e^{-1.83\tau} + 0.0006803033077\hbar^2 e^{-1.67\tau} +$$

$$+ 2.249178162 \cdot 10^{-6} \hbar^2 e^{-1.25\tau} + 2.516222247 \cdot 10^{-13} \hbar^2 e^{-0.49\tau} - 3.256784872 \cdot 10^{-8} \hbar^2 e^{0.09\tau} + 0.002025850052 \hbar^2, \quad (46)$$

$$A(\tau) = 10 - 10e^{-\tau} - 1.717948718\hbar + 4.02000000\hbar e^{-1.34\tau} - 2.302051282\hbar e^{-2.34\tau} + 0.000935423077\hbar^2 \tau - 0.2499344656\hbar^2 - 0.0007177972977\hbar^2 e^{-2.34\tau} + 0.1156579541\hbar^2 e^{-1.34\tau} - 0.02423181662\hbar^2 e^{-4.01\tau} - 0.2723883412\hbar^2 e^{-3.68\tau} - 0.0001052461055\hbar^2 e^{-3.59\tau} + 0.1155576208\hbar^2 e^{-3.01\tau} + 0.3164745002\hbar^2 e^{-2.68\tau} + 0.0002674497236\hbar^2 e^{-2.59\tau} - 1.348557517 \cdot 10^{-6} \hbar^2 e^{-2.25\tau} - 0.15477\hbar^2 e^{-2.01\tau} - 0.04319386084\hbar^2 e^{-1.67\tau} + 4.450239808 \cdot 10^{-6} \hbar^2 e^{-1.25\tau} + 0.1973809015\hbar^2 e^{-0.67\tau}. \quad (47)$$

The above solution is for  $M = 2$ . We have obtained a fifth-order solution using Maple. Moreover, we can find higher-order solutions until the solution converges [Naik, Zu, Ghoreishi, 2020a; Noeiaghdam, Suleman, Budak, 2018]. The approximate solution at fifth order gives an error of about 1.03 %. We can further extend for next iterations in order to obtain a more approximate solution. It is important to ensure the convergence of the series (45)–(47). The auxiliary parameter  $\hbar$  plays a key role in the solution series convergence and its accuracy. We have plotted  $\hbar$ -curves for the variables and its derivatives for a particular value of  $\tau$  in Figs. 4–6. The valid region of  $\hbar$  can be discovered from these curves, which corresponds to the nearly parallel line segment to the horizontal axis. The valid regions are presented in Table 2.

## 4. Results and Discussion

Equations (45)–(47) represent the analytical expression of the system (5)–(8). This solution is extended up to fifth order using Maple. The numerical simulation is computed in Matlab. The graphs of analytical approximation series are compared with numerical simulation to show the validation of the approximate solution. For the analysis, we assume that the number of coconut leaves is as 7, the number of whitefly eggs per leaf is 200 and that of predator eggs is 0 initially. Thus, the initial values of the system are considered as  $E(0) = 7$ ,  $F(0) = 200$ ,  $G(0) = 0$ . Based on this, the initial conditions of the nondimensional system are calculated as  $L(0) = 0.03$ ,  $W(0) = 0.67$ ,  $A(0) = 0$ . The fecundity rate of predator, its death rate based on the number of eggs hatched and the predation rate are calculated by using the data given in [Rao, Ramani, Bhagavan, 2020; Chalapathi Rao et al., 2022]. The fecundity rate of whitefly and its death rate are calculated based on the data given in [Elango, Nelson, Aravind, 2020].

Figure 1 interprets that, when the value of  $f$  is increased, there is an increase in the growth of coconut leaves. From Figure 2, we see that the increase in  $n$  and  $p$  decreases the whitefly population. Figure 3 shows that the increase in  $q$  leads to an increase in predator population. Figure 4 represents the  $\hbar$ -curve of the fifth-order solution of  $L(\tau)$  at  $\tau = 0.5$  where the horizontal line denotes the convergence region. Figures 5 and 6 represent the  $\hbar$ -curve of fifth-order solution of  $W(\tau)$  at  $\tau = 0.6$  and  $A(\tau)$  at  $\tau = 0.01$  respectively. Figure 7 shows a pictorial representation of the fifth-order approximate analytical solution of the system. Figure 8 infers the surface plot for (a)  $L(\tau)$  with respect to  $f$  and time, (b) whitefly population  $W(\tau)$  for  $p$  and time (c)  $A(\tau)$  with respect to  $q$  and time. The parametric values used for the analysis are given in Table 1. The valid range for  $\hbar$  is given in Table 2. The error approximation is obtained by comparing the HAM result and numerical simulation result of Eq. 5 in Table 3. The error approximation by comparing the HAM result and numerical simulation result of Eq. 6 is represented in Table 4 and Table 5. The error approximation by comparing the HAM result and numerical simulation result of Eq. 7 is given in Table 6. HAM provides us with a great deal of freedom in developing the solution for nonlinear problems. This provides various benefits which are not available in ordinary perturbation methods. The  $\hbar$ -curves clearly show the admissible region of  $\hbar$  with which we obtain the convergence of solution series. Thus, the results obtained by HAM seem

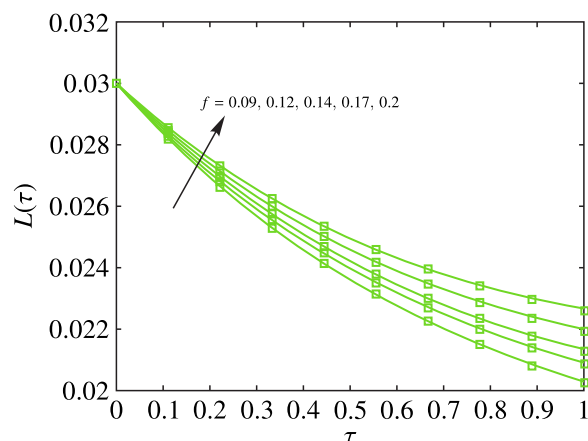


Figure 1. Profile of  $L(\tau)$  versus time by using the HAM solution and numerical simulation for  $n = 0.67$ ,  $m = 0.01$ ,  $p = 0.063$ ,  $q = 0.6$ ,  $g = 10$ ,  $\hbar = -1$ ,  $u = 0.33$ . The curves denoted by — represent numerical simulation and  $\square$  represent HAM solution (Eq. 45)

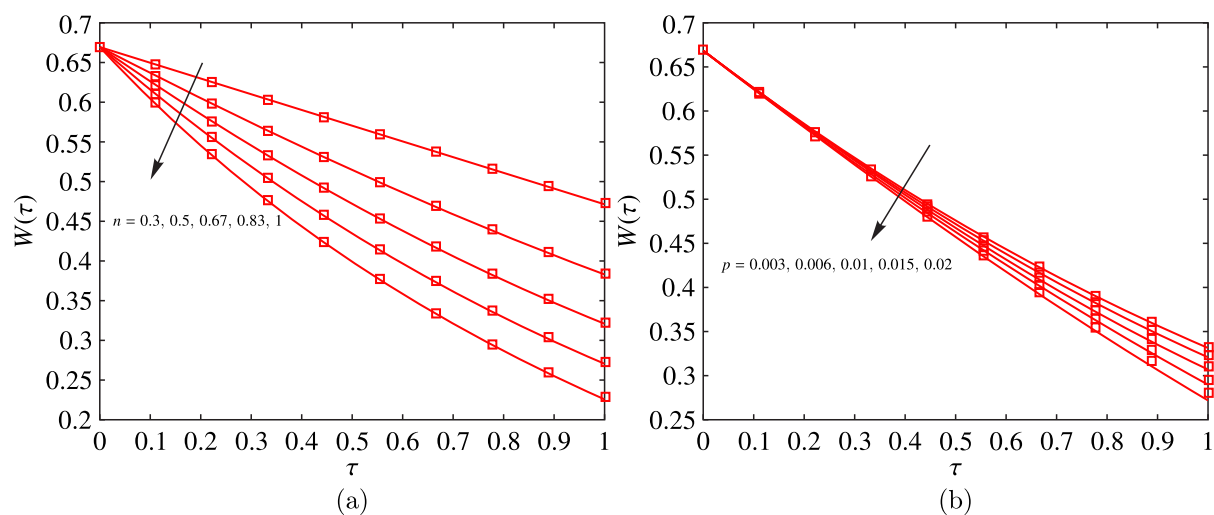


Figure 2. Profile of  $W(\tau)$  versus time by using the HAM solution and numerical simulation for the values (a)  $f = 0.09$ ,  $m = 0.01$ ,  $p = 0.063$ ,  $q = 0.6$ ,  $g = 10$ ,  $u = 0.33$ ,  $\hbar = -2.5$ ; (b)  $f = 0.09$ ,  $m = 0.01$ ,  $q = 0.6$ ,  $g = 10$ ,  $u = 0.33$ ,  $\hbar = -2.5$ . The curves denoted by — represent numerical simulation and  $\square$  represent HAM solution (Eq. 46)

to be trustworthy as they agree with numerical simulation results and the maximum error percentage is 1.03 %.

## 5. Conclusion

In this paper, the nonlinear ordinary differential equation model describing the interaction of rugose spiraling whitefly, a major pest in coconut trees with its natural predator, *Pseudomallada astur*, has been discussed. The predation rate is considered as Holling type III functional response. The model interprets that the use of predator can efficiently control the whitefly population. The approximate analytical solution is obtained for the system by using HAM and we have represented the solution in terms of the base functions that most closely approximate the behavior of the problem's actual solution. The convergence and accuracy of the solution series is controlled by the auxiliary parameter  $\hbar$  which is one of the important features that other methods do not possess. Thus, several  $\hbar$ -curves have



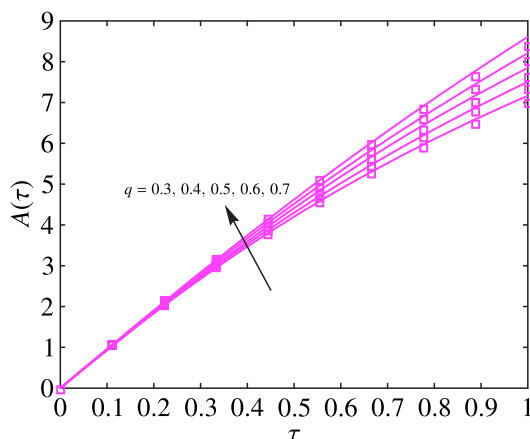


Figure 3. Profile of  $A(\tau)$  versus time by using the HAM solution and numerical simulation for  $f = 0.09$ ,  $m = 0.01$ ,  $p = 0.063$ ,  $g = 10$ ,  $u = 0.33$ ,  $\hbar = -2.8$ ,  $n = 0.67$ . The curves denoted by — represent numerical simulation and  $\square$  represent the HAM solution of (Eq. 47)

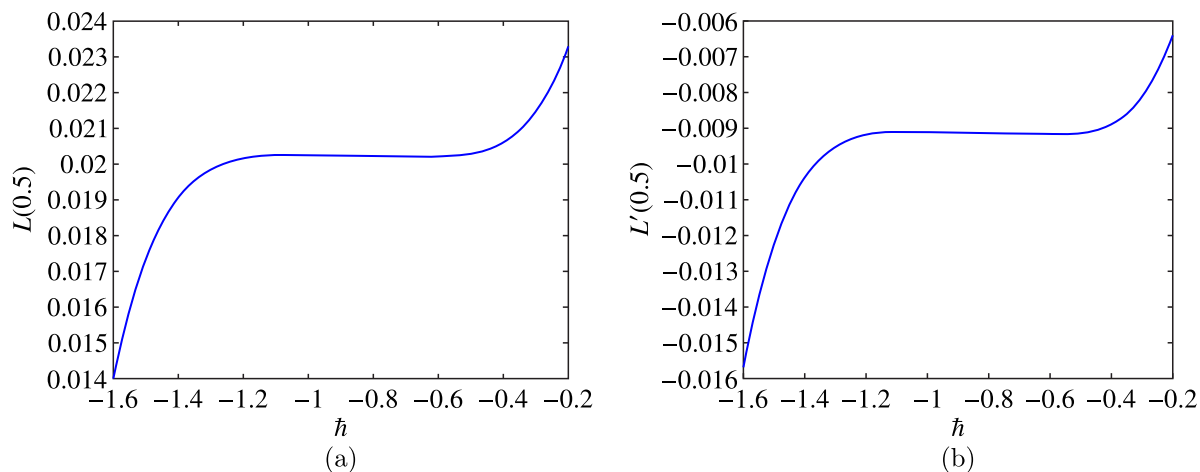


Figure 4.  $\hbar$  curves for the fifth-order solution of (a)  $L(\tau)$ , (b)  $L'(\tau)$  at  $\tau = 0.5$

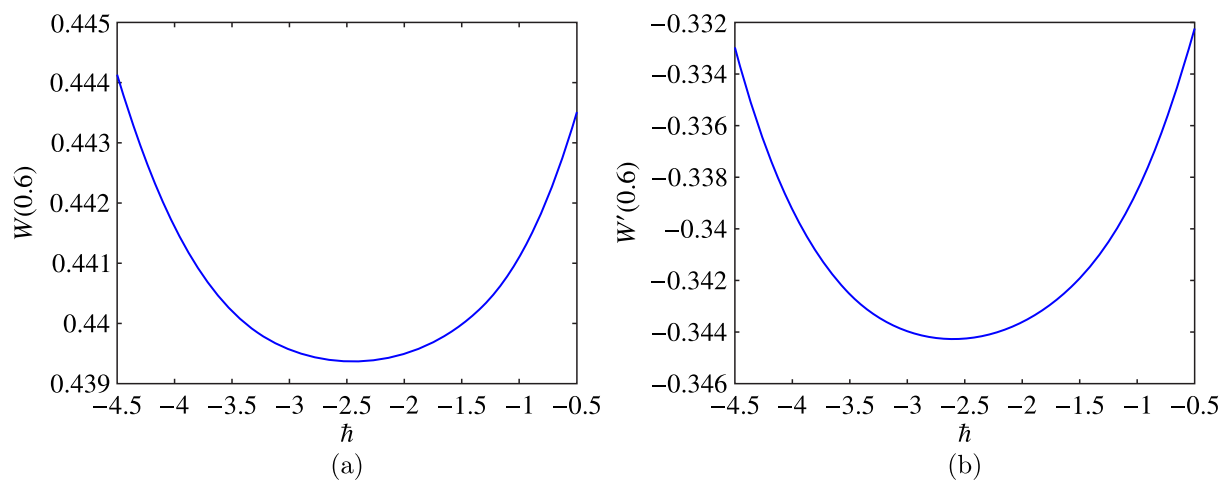


Figure 5.  $\hbar$  curves for the fifth-order solution of (a)  $W(\tau)$ , (b)  $W'(\tau)$  at  $\tau = 0.6$

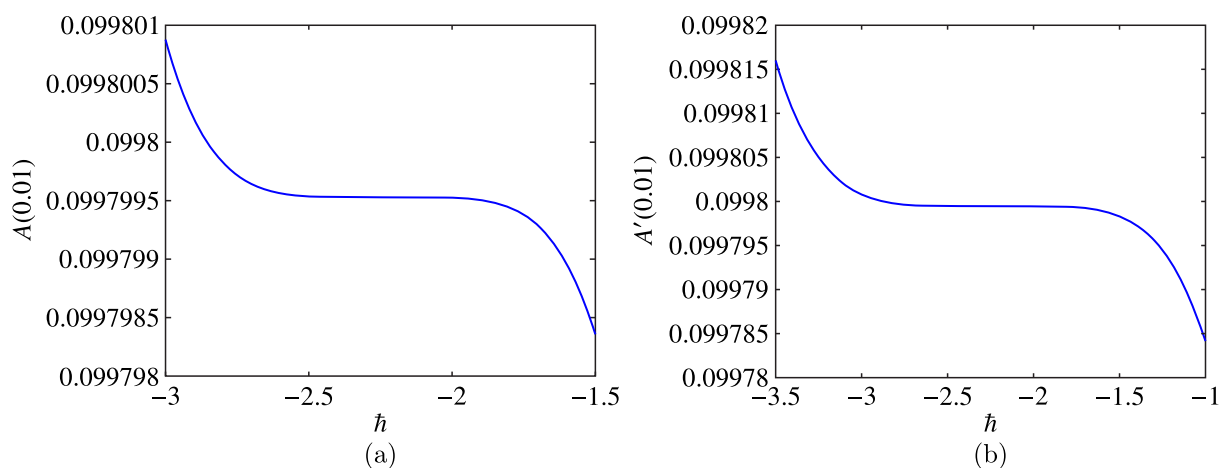


Figure 6.  $h$  curves for the fifth-order solution of (a)  $A(\tau)$ , (b)  $A'(\tau)$  at  $\tau = 0.01$

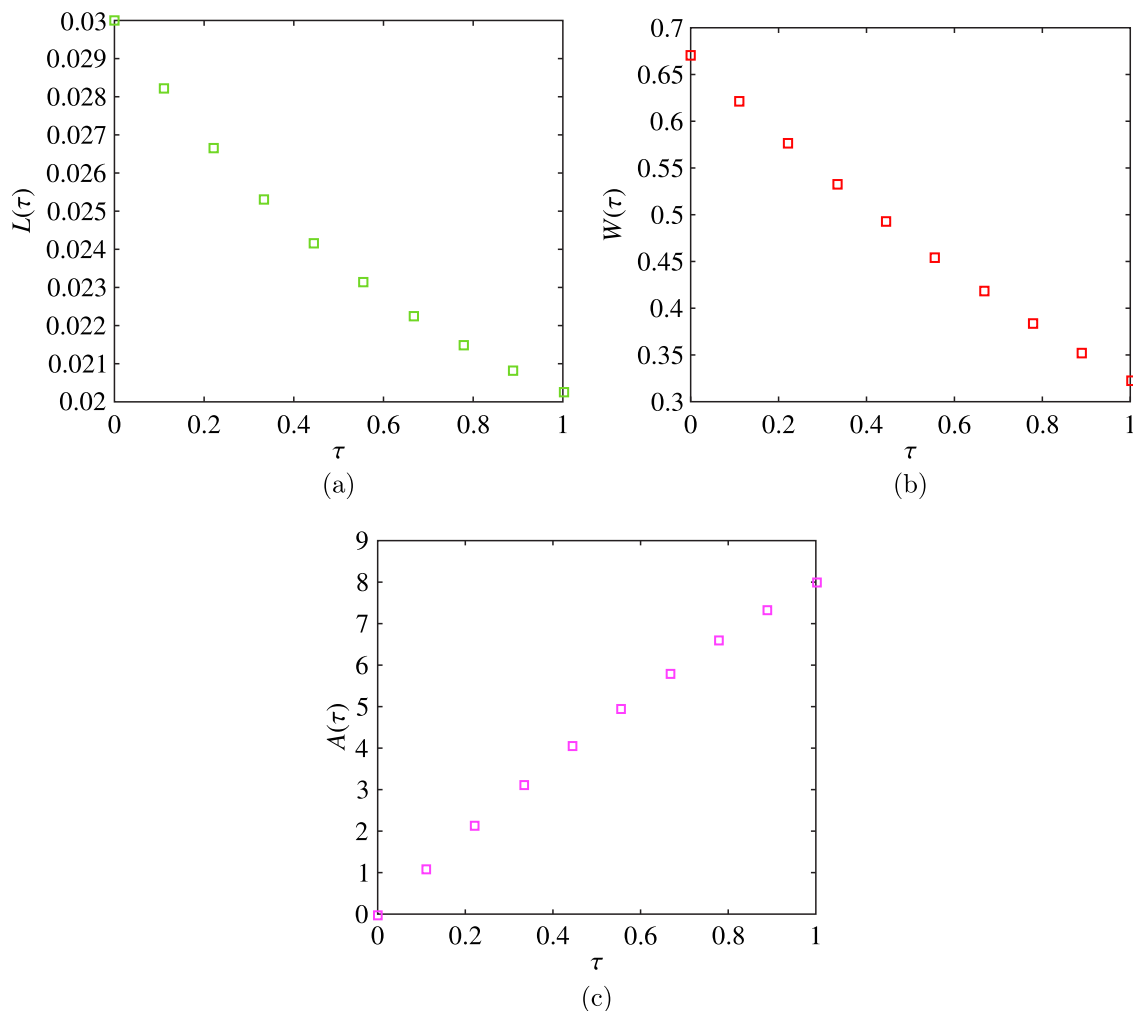


Figure 7. Pictorial representation of the approximate analytical solution of the system at fifth order (a)  $L(\tau)$ , (b)  $W(\tau)$ , (c)  $A(\tau)$  for the parametric values  $n = 0.67$ ,  $m = 0.01$ ,  $p = 0.063$ ,  $q = 0.6$ ,  $g = 10$ ,  $u = 0.03$ ,  $f = 0.09$  and corresponding  $h$  values

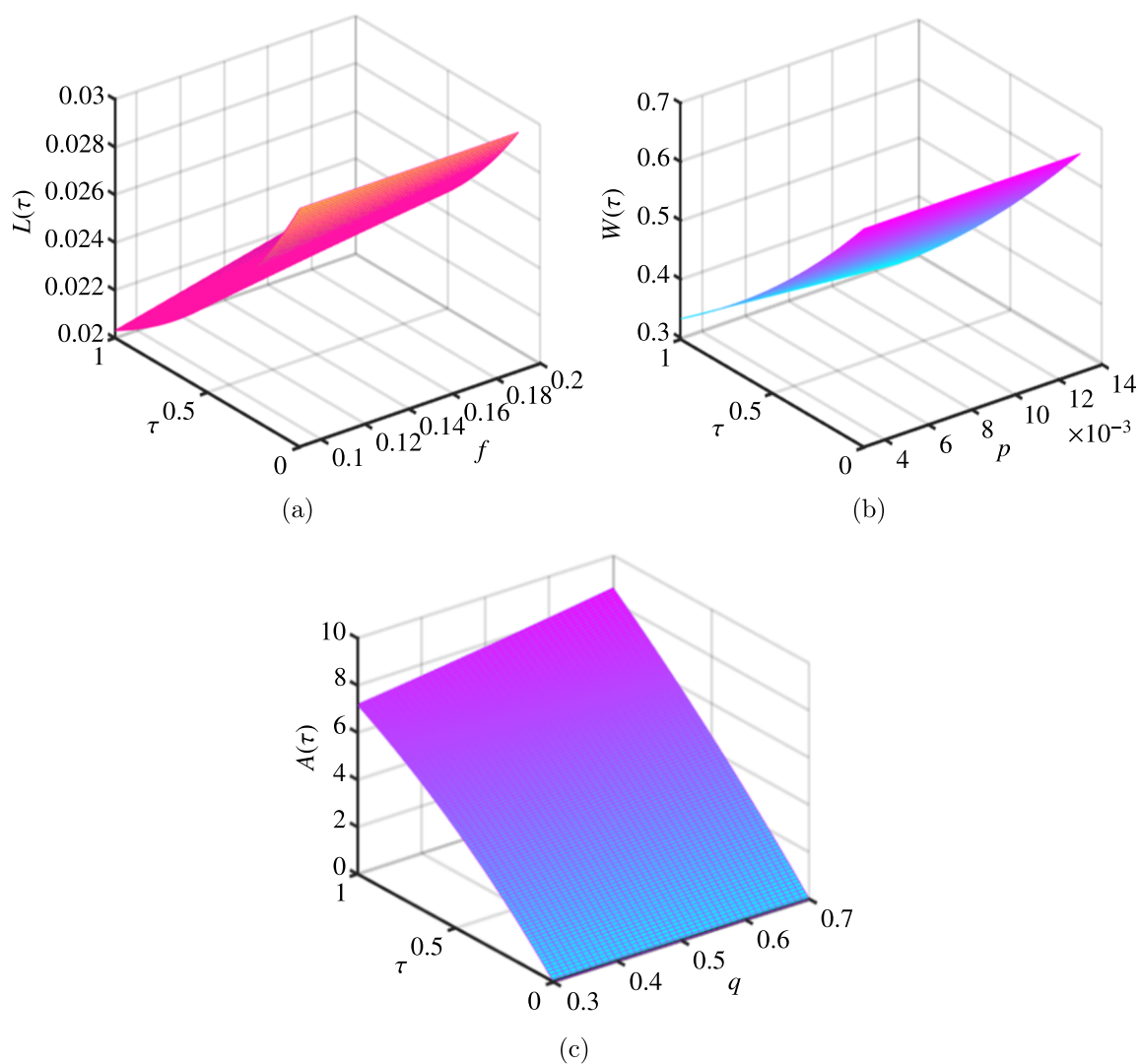


Figure 8. Surface plot of (a) coconut leaves with respect to time and  $f$ , (b) whitefly eggs with respect to time and  $p$ , (c) predator eggs with respect to time and  $q$

Table 1. Parametric values used for the analysis

S. No	Symbol	Meaning	Values
1	$r$	Growth rate of coconut leaves	0.0027–0.004 day <sup>-1</sup>
2	$\alpha$	Infection rate	0.00001–0.0005 pest <sup>-1</sup> day <sup>-1</sup>
3	$\beta$	Growth rate of the whitefly	0.02–0.04 day <sup>-1</sup>
4	$a$	Predation rate	0.019 predator <sup>-1</sup> day <sup>-1</sup>
5	$b$	Half saturation constant	10
6	$\zeta$	Death rate of the whitefly	0.01–0.025 day <sup>-1</sup>
7	$c$	Growth rate of the predator	0.58–0.78 day <sup>-1</sup>
8	$\omega$	Death rate of the predator	0.02–0.04 day <sup>-1</sup>
9	$\eta$	Predator eggs added	10

been plotted and the region of convergence is shown. The approximate analytical results are in good agreement with the numerical simulation results.

Table 2. The admissible range of  $\hbar$  obtained from Figure 4–6

Variables	$\hbar$ range
$L(\tau)$	$-1 \leq \hbar \leq -0.8$
$W(\tau)$	$-2.8 \leq \hbar \leq -2.3$
$A(\tau)$	$-2.8 \leq \hbar \leq -2$

Table 3. Comparison of numerical results and the HAM solution of (Eq. 45) for various values of  $f$  and other parameters as in Figure 1

$\tau$	$f = 0.09$			$f = 0.14$			$f = 0.17$			$f = 0.2$		
	Numerical	HAM	Error %	Numerical	HAM	Error %	Numerical	HAM	Error %	Numerical	HAM	Error %
0	0.02999	0.02998	0.03334	0.02999	0.02999	0.00000	0.02999	0.02999	0.00000	0.02999	0.02999	0.00000
0.2	0.02695	0.02695	0.00754	0.02722	0.02723	0.03083	0.02738	0.02739	0.03164	0.02755	0.02755	0.02529
0.4	0.02459	0.02459	0.00852	0.02509	0.02510	0.03674	0.02539	0.02540	0.03983	0.02570	0.02570	0.02765
0.6	0.02278	0.02277	0.04453	0.02347	0.02347	0.00828	0.02390	0.02390	0.01476	0.02433	0.02433	0.00306
0.8	0.02139	0.02136	0.12216	0.02226	0.02225	0.06268	0.02280	0.02278	0.05222	0.02335	0.02333	0.07592
1	0.02029	0.02024	0.24641	0.02133	0.02129	0.18282	0.02198	0.02194	0.16834	0.02265	0.02261	0.19865
	Mean Error %		0.00771	Mean Error %		0.05356	Mean Error %		0.05113	Mean Error %		0.05509

Table 4. Comparison of numerical results and the HAM solution of (Eq. 46) for various values of  $n$  and other parameters as in Figure 2

$\tau$	$n = 0.3$			$n = 0.5$			$n = 0.83$			$n = 0.1$		
	Numerical	HAM	Error %	Numerical	HAM	Error %	Numerical	HAM	Error %	Numerical	HAM	Error %
0	0.67000	0.67000	0.00000	0.67000	0.67000	0.00000	0.67000	0.66990	0.01493	0.66990	0.66980	0.01493
0.2	0.62982	0.62986	0.00590	0.60509	0.60517	0.01355	0.56648	0.56652	0.00647	0.54752	0.54760	0.01328
0.4	0.58973	0.58981	0.01355	0.54413	0.54425	0.02114	0.47650	0.47658	0.01535	0.44490	0.44504	0.03276
0.6	0.54990	0.55010	0.03736	0.48695	0.48721	0.05335	0.39840	0.39875	0.08767	0.35911	0.35964	0.14799
0.8	0.51046	0.51095	0.09614	0.43333	0.43401	0.15622	0.33052	0.33172	0.36457	0.28726	0.28890	0.57163
1	0.47158	0.47259	0.21481	0.38310	0.38462	0.39865	0.27119	0.27417	1.09886	0.22644	0.23033	1.71789
	Mean Error %		0.06129	Mean Error %		0.10715	Mean Error %		0.26464	Mean Error %		0.41641

Table 5. Comparison of numerical results and the HAM solution of (Eq. 46) for various values of  $p$  and other parameters as in Figure 2

$\tau$	$p = 0.003$			$p = 0.006$			$p = 0.01$			$p = 0.02$		
	Numerical	HAM	Error %	Numerical	HAM	Error %	Numerical	HAM	Error %	Numerical	HAM	Error %
0	0.67000	0.66990	0.01492	0.67000	0.66990	0.01493	0.67000	0.66990	0.01493	0.67000	0.66980	0.02985
0.2	0.58549	0.58546	0.00604	0.58492	0.58492	0.00073	0.58417	0.58422	0.00841	0.58230	0.58236	0.01129
0.4	0.51048	0.51046	0.00292	0.50839	0.50839	0.00041	0.50563	0.50569	0.01147	0.49872	0.49879	0.01467
0.6	0.44395	0.44401	0.01380	0.43959	0.43975	0.03583	0.43378	0.43419	0.09422	0.41929	0.42045	0.27608
0.8	0.38493	0.38522	0.07611	0.37770	0.37840	0.18550	0.36806	0.36964	0.43018	0.34403	0.34869	1.35286
1	0.33242	0.33320	0.23464	0.32190	0.32377	0.58093	0.30788	0.31194	1.31999	0.27296	0.28486	4.35904
	Mean Error %		0.05807	Mean Error %		0.13639	Mean Error %		0.31320	Mean Error %		1.00729

## Conflict of Interest

The authors declare that there is no conflict of interest.

## Acknowledgements

The authors are very much thankful to the management, SRM Institute of Science and Technology for their continuous support and encouragement.

Table 6. Comparison of numerical results and the HAM solution of (Eq. 47) for various values of  $q$  and other parameters as in Figure 3

$\tau$	$q = 0.3$			$q = 0.4$			$q = 0.5$			$q = 0.6$		
	Numerical	HAM	Error %	Numerical	HAM	Error %	Numerical	HAM	Error %	Numerical	HAM	Error %
0	0.00005	0.00005	0.00000	0.00003	0.00003	0.00000	0.00002	0.00002	0.00000	0.00001	0.00001	0.00000
0.2	1.86545	1.86447	0.05257	1.88393	1.88268	0.06650	1.90259	1.90102	0.08269	1.92149	1.91959	0.09878
0.4	3.48866	3.47849	0.29148	3.55555	3.54529	0.28884	3.62419	3.61387	0.28489	3.69489	3.68463	0.27793
0.6	4.89805	4.85993	0.77837	5.03654	4.99674	0.79013	5.18031	5.13879	0.80149	5.33030	5.28700	0.81233
0.8	6.12147	6.02508	1.57467	6.34815	6.24439	1.63456	6.58621	6.47419	1.70080	6.83761	6.71621	1.77546
1	7.18677	6.99025	2.73442	7.51168	7.29557	2.87699	7.85715	7.61846	3.03778	8.22675	7.96178	3.22091
	Mean Error %		0.90525	Mean Error %		0.94284	Mean Error %		0.98461	Mean Error %		1.03090

## References

- Allen L. J., Brauer F., Van den Driessche P., Wu J. *Mathematical epidemiology*. — Berlin: Springer, 2008.
- Chalapathi Rao N. B. V., Ramani B. S. L., Roshan D. R., Bhagavan B. V. K. Diet standardization for Pseudomallada astur Banks (Neuroptera: Chrysopidae) and assessment of its predatory potential against the rugose spiralling whitefly Aleurodicus rugioperculatus Martin (Hemiptera: Aleyrodidae) // *International Journal of Tropical Insect Science*. — 2022. — Vol. 42, No. 1. — P. 783–791.
- Elango K. Biology, distribution and host range of new invasive pest of India coconut rugose spiralling whitefly Aleurodicus rugioperculatus Martin in Tamil Nadu and the status of its natural enemies // *International Journal of Agriculture Sciences*. — 2019.
- Elango K., Nelson S. J., Aravind A. Rugose spiralling whitefly, Aleurodicus rugioperculatus Martin (Hemiptera, Aleyrodidae): An invasive foes of coconut // *Journal of Entomological Research*. — 2020. — Vol. 44, No. 2. — P. 261–266.
- Holt J., Jeger M. J., Thresh J. M., Otim-Nape G. W. An epidemiological model incorporating vector population dynamics applied to African cassava mosaic virus disease // *Journal of Applied Ecology*. — 1997. — P. 793–806.
- Liao S. An explicit analytic solution to the Thomas–Fermi equation // *Applied Mathematics and Computation*. — 2013. — Vol. 144, No. 2–3. — P. 495–506.
- Liao S. *Beyond perturbation: introduction to the homotopy analysis method*. — CRC press, 2003.
- Liao S. On the homotopy analysis method for nonlinear problems // *Applied Mathematics and Computation*. — 2004. — Vol. 147, No. 2. — P. 499–513.
- Naik P. A., Zu J., Ghoreishi M. Estimating the approximate analytical solution of HIV viral dynamic model by using homotopy analysis method // *Chaos, Solitons & Fractals*. — 2020a. — Vol. 131. — P. 109500.
- Naik P. A., Zu J., Ghoreishi M. Stability analysis and approximate solution of SIR epidemic model with Crowley–Martin type functional response and holling type II treatment rate by using homotopy analysis method // *Journal of Applied Analysis & Computation*. — 2020b. — Vol. 10, No. 4. — P. 1482–1515.
- Noeiaghdam S., Suleman M., Budak H. Solving a modified nonlinear epidemiological model of computer viruses by homotopy analysis method // *Mathematical Sciences*. — 2018. — Vol. 12, No. 3. — P. 211–222.
- Pathak S., Maiti A. Pest control using virus as control agent: A mathematical model // *Nonlinear Analysis: Modelling and Control*. — 2012. — Vol. 17, No. 1. — P. 67–90.

- Rao N. C., Ramani B., Bhagavan B.* Functional response and density dependent feeding interaction of *Pseudomallada astur* Banks (Neuroptera: Chrysopidae) against Rugose spiraling whitefly, *Aleurodicus rugioper culatus* Martin (Hemiptera: Aleyrodidae) // *Pest Management in Horticultural Ecosystems*. — 2020. — Vol. 26, No. 2. — P. 229–234.
- Shirkhani M. R., Hoshyar H. A., Rahimipetroudi I., Akhavan H., Ganji D. D.* Unsteady time-dependent incompressible Newtonian fluid flow between two parallel plates by homotopy analysis method (HAM), homotopy perturbation method (HPM) and collocation method (CM) // *Propulsion and Power Research*. — 2018. — Vol. 7, No. 3. — P. 247–256.
- Suganya G., Senthamarai R.* Mathematical modeling and analysis of Phytoplankton–Zooplankton–Nanoparticle dynamics // *Mathematical Modeling and Computing*. — 2022a. — Vol. 9, No. 2. — P. 333–341.
- Suganya G., Senthamarai R.* Mathematical modeling and analysis of the effect of the rugose spiraling whitefly on coconut trees // *AIMS Mathematics*. — 2022b. — Vol. 7, No. 7. — P. 13053–13073.
- Sundararaj R., Selvaraj K.* Invasion of rugose spiraling whitefly, *Aleurodicus rugioperculatus* Martin (Hemiptera: Aleyrodidae): a potential threat to coconut in India // *Phytoparasitica*. — 2017. — Vol. 45, No. 1. — P. 71–74.